Journal of Catalysis 275 (2010) 294–299

Contents lists available at ScienceDirect

Journal of Catalysis

journal homepage: www.elsevier.com/locate/jcat

Effect of water on formic acid photocatalytic decomposition on TiO_2 and Pt/TiO_2

Kristi L. Miller [a], Chul Woo Lee [b], John L. Falconer [a], J. Will Medlin [a,*]

[a] Department of Chemical and Biological Engineering University of Colorado, Boulder, CO 80309-0424, United States
[b] Department of Chemical Engineering, Hanbat National University, Daejeon 305-719, South Korea

ARTICLE INFO

Article history:
Received 19 May 2010
Revised 11 August 2010
Accepted 20 August 2010
Available online 28 September 2010

Keywords:
Photocatalysis
Formic acid
TiO_2
Water
Fourier transform infrared spectroscopy (FTIR)

ABSTRACT

The effect of water on the adsorption and photocatalytic decomposition (PCD) of formic acid on TiO_2 and Pt/TiO_2 was investigated using transient reaction studies, temperature-programmed desorption (TPD), and Fourier transform infrared (FTIR) spectroscopy. Reaction studies indicated that physisorbed water increased the PCD rate of formic acid to a small extent on TiO_2 and to a major extent on Pt/TiO_2, but the presence of only chemisorbed water did not. FTIR spectroscopy and TPD studies indicate that the main effect of the addition of water to TiO_2 that had adsorbed formic acid was the displacement of formic acid. However, FTIR spectroscopy indicated that the addition of water caused a change in the adsorbed structure of formate that may be associated with the higher reactivity. These transformations can have an important influence on elementary steps in the photocatalytic decomposition of formic acid on TiO_2 and Pt/TiO_2.

1. Introduction

Titania photocatalytically oxidizes low concentrations of organics at room temperature, and the anatase form of TiO_2 has a higher activity than the rutile form [1]. Photocatalytic reactions clean waste air streams and indoor air, and are used for self-cleaning windows. Ultraviolet light initiates reaction by exciting electrons from the valence to the conduction band of a semiconductor to create an electron–hole pair. On TiO_2, the hole oxidizes formic acid, sometimes completely to CO_2 and H_2O in the presence of oxygen (photocatalytic oxidation, PCO), or it decomposes formic acid to CO_2 and H_2O by extracting a lattice oxygen in the absence of oxygen (photocatalytic decomposition, PCD). On Pt/TiO_2, formic acid decomposes to CO_2 and H_2 during PCD.

Water, which is usually present during photocatalytic reactions, promotes or inhibits reaction rates, depending on the reactant and water concentrations, and thus the influence of water on species adsorbed on TiO_2 is of interest [2–8]. Multiple studies show that water increases the PCO and PCD rates of formic acid, but the reasons for the rate increase are unclear [9–12]. Liao et al. [9] observed from IR spectroscopy that the rate of formic acid and formate PCO increased by a factor of two when water was above 60% saturation coverage, indicating the $H_2O(a)/HCOO(a)$ ratio must reach a certain value for water to substantially increase the photooxidation rate. The optimum water concentration is vital because previous work has shown that when the water concentration is too high, competitive adsorption decreases the photocatalytic rate [6,8,13].

In the current study, the accelerating effect of water was investigated in transient photocatalytic decomposition experiments with formic acid. Both TiO_2 and Pt/TiO_2 catalysts were employed as catalysts. Weakly adsorbed water was found to have a significant effect on PCD rate, but strongly chemisorbed water did not. One possible mechanism for this rate acceleration is that coadsorbed water changes the configuration of formic acid adsorbed on TiO_2. For example, Vittadini et al. used DFT calculations to show that water induces the dissociation of formic acid to formate on anatase (1 0 1) [14]. To probe this possibility, we used Fourier transform infrared spectroscopy (FTIR) and temperature-programmed desorption (TPD). The FTIR and TPD measurements were applied to high surface area P25 TiO_2 (80% anatase and 20% rutile).

2. Experimental methods

2.1. Reaction studies

For room-temperature PCD experiments, a thin layer of 45 mg of P25 TiO_2 (80% anatase and 20% rutile) or 30 mg of Pt/TiO_2 catalyst was coated on the inner side of an annular Pyrex reactor to ensure that UV lights irradiated the entire catalyst surface. The average film thickness was calculated to be 0.4 μm. To provide adequate catalyst surface area with these thin films, the outer diameter of the reactor was 2 cm and the reactor was 13 cm long. The reactor consisted of two concentric cylinders that formed an annular region with a 1-mm gap; the inner cylinder was evacuated

* Corresponding author. Fax: +1 303 492 4341.
E-mail address: will.medlin@colorado.edu (J.W. Medlin).

0021-9517/$ - see front matter © 2010 Elsevier Inc. All rights reserved.
doi:10.1016/j.jcat.2010.08.011

and sealed. A diagram of the apparatus has been previously presented [15]. The annular reactor ensured a high gas flow rate through the reactor, but allowed for a larger diameter reactor. High flow rates guaranteed quick detection of products desorbing from the surface. A thermocouple located on the inside of the reactor recorded the catalyst temperature.

A 0.2 wt.% Pt/TiO_2 was prepared using 67 mg of H_2PtCl_6 mixed with 10 g Degussa P25 TiO_2 in 100 ml HCl. First, Na_2CO_3 was added until a pH of 7–8, and then 3 mL of acetic acid was added until the solution reached a pH of 4. Next, 300 mL of water was added, and N_2 was bubbled through the solution under an UV lamp for 6 h. The solution was filtered and washed with H_2O. The catalyst was then dried at 373 K for 24 h and coated on the inside of the reactor by evaporative deposition of a sonicated slurry of catalyst and water. Twelve 8-W UV lamps (BLB Korea, type F8T5BLB), placed in a circle 6 cm from the reactor, radiated the reactor. Radiometer measurements showed a UV intensity of 2.5 mW cm^{-2} and a maximum light intensity at 360 nm. Turning the lights on and off started and stopped the PCD reaction.

A quartz tube furnace held the catalyst temperature at 723 K for 30 min in a 20% O_2/80% He stream to remove hydrocarbons and deposits from previous reactions. The transparent furnace allowed for the transmission of UV light during heating and cooling of the reactor. The reactor was cooled to room temperature, and 2 μL of liquid formic acid (Aldrich, 99%) was injected into the reactor. For experiments with co-adsorbed water, 2 μL of a mixture of formic acid and distilled water was injected. The reactor was flushed for 2 h, and then turning on the UV lights initiated isothermal reaction at room temperature. For experiments with physisorbed water, 1 μL of water was injected during PCD. During transient PCD, 100 cm^3 min^{-1} (STP) of He or Ar flowed through the reactor, and a Balzers quadrupole mass spectrometer (QMA 125) detected products as a function of time. A computer recorded the amplitudes of multiple mass peaks and the catalyst temperature simultaneously. Known volumes of gases injected downstream from the reactor were used to calibrate the mass spectrometer. The O_2 concentration in the feed stream, estimated be 0.3 ppm, remained below the detection limit of the mass spectrometer [16]. After PCD, TPD (He or Ar flow) and TPO (20% O_2 flow) were performed by heating the catalyst to 723 K at a rate of 1 K s^{-1} while monitoring the mass signals with the mass spectrometer.

2.2. Infrared spectroscopy

A Nicolet 6700 FT-IR Spectrometer recorded infrared spectra at 4 cm^{-1} resolution. Titania samples were prepared by pressing Degussa P25 TiO_2 powder into a tungsten grid with a hydraulic press. A chromel–alumel thermocouple spot-welded to the tungsten grid measured the temperature, and the grid was attached to a copper holder and placed in a small stainless steel vacuum chamber with CaF_2 windows for the IR beam. The TiO_2 catalyst was cleaned by heating in vacuum for 4 h at 673 K and then in oxygen at 473 K for 2 h. Formic acid was adsorbed by exposing the sample to saturated vapor at room temperature. The cell was then evacuated for 20 min to remove weakly adsorbed formic acid. Saturated water was added to the cell at room temperature, and IR spectra were recorded at various water pressures as water was slowly removed from the system. The IR spectra for gas-phase water was subtracted from the IR spectra recorded to correct for water in the gas phase.

2.3. Temperature-programmed desorption

A packed-bed tubular reactor (7-mm i.d.) was used for TPD and TPO measurements. The catalyst (106 mg of Degussa P25 TiO_2) was placed on quartz wool, which rested on a quartz frit in a quartz reactor. A chromel–alumel thermocouple was placed in the center of the catalyst bed, and a temperature controller was used to control a quartz tube furnace that ramped the catalyst temperature from room temperature to 723 K at 1 K s^{-1}. The temperature was not increased above 723 K to avoid a phase change to rutile. A Balzers quadrupole mass spectrometer sampled the effluent from the reactor through a silica capillary. Before each experiment, the TiO_2 sample was oxidized for 30 min at 723 K in a 20% O_2/80% He stream, and then cooled to room temperature. During TPD, helium flowed through the reactor at a rate of 100 cm^3 (STP) min^{-1}. Liquid formic acid and water were injected upstream of the room-temperature catalyst with a syringe, and the liquids evaporated in the flowing stream so that only vapor contacted the catalyst. A TPD to 723 K was performed 1 h after the last injection. For calibration, known amounts of formic acid, water, and carbon monoxide were injected into the gas stream below the reactor.

3. Results

3.1. Photocatalytic decomposition of formic acid on TiO_2 and Pt/TiO_2

During transient PCD at room temperature, physisorbed water increased the rate of formic acid decomposition on both TiO_2 and Pt/TiO_2. On TiO_2, the CO_2 formation rate only increased by 25% (Fig. 1), whereas on Pt/TiO_2, *the CO_2 formation rate increased a factor of 8*, as shown in Fig. 2. During the initial period of the reaction in this transient experiment, the reaction rate decays exponentially as the coverage of formic acid on the catalyst decreases due to reaction. Water was injected upstream of the reactor after 310 s of PCD; at that time, the rate was 15% of its initial value. Water increased the PCD rate a factor of eight, and it increased the rate above the rate for the initially saturated surface, even though the formic acid coverage was significantly lower after 310 s of reaction. In a separate experiment, water and formic acid were co-adsorbed and the reactor flushed before PCD. The PCD rate was essentially the same as for formic acid alone. Water that remained adsorbed in the absence of gas-phase water did not accelerate the PCD rate on Pt/TiO_2. Physisorbed water apparently enhanced the formic acid PCD rate, but strongly adsorbed water did not. Liao et al. [9] did not distinguish between physisorbed and chemisorbed water, but determined that 60% saturation coverage of water was required to increase the formic acid PCO rate on TiO_2.

The mechanism for the acceleration of the PCD rate by water is not immediately clear. There are many complex aspects of surface chemistry; for example, the P25 catalyst consists of a mixture of TiO_2 crystal structures (80% anatase and 20% rutile), and even

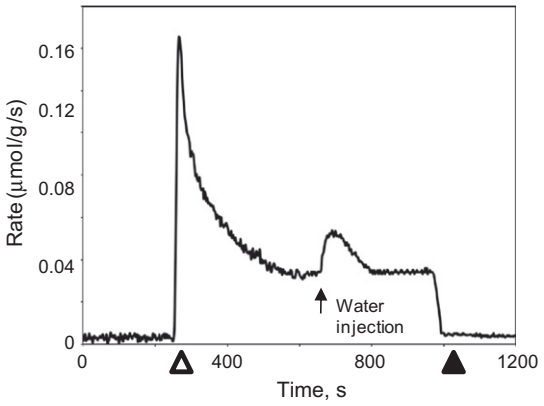

Fig. 1. The CO_2 formation rate during formic acid PCD on TiO_2. The UV lights were turned on (open triangles) and off (solid triangles) as indicated. Water was injected after 650 s.

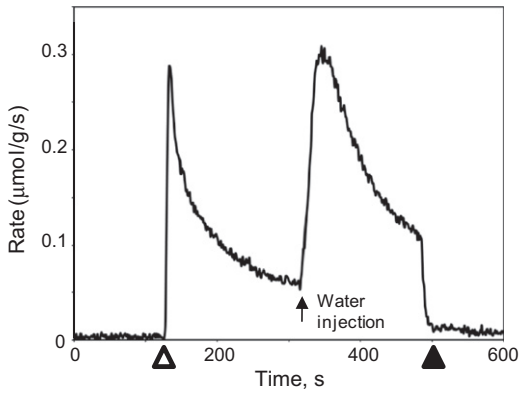

Fig. 2. The CO_2 formation rates during formic acid PCD on Pt/TiO_2. The UV lights were turned on (open triangles) and off (solid triangles) as indicated. Water was injected after 310 s.

within a single type of crystal, multiple facets will be exposed at the surface. Furthermore, the accelerating effect of water is much greater on Pt/TiO_2, suggesting that chemistry at Pt–TiO_2 interfaces may be important to the mechanism. To make progress in investigating how water may play a role in this and other related reactions, the investigations below focus on the effect of water on the adsorbed states of formic acid and a key initial decomposition intermediate, formate, on TiO_2. In simulations, TiO_2 is in most cases modeled as an anatase (1 0 1) single crystal, the most abundant crystal face, and the role of Pt is not directly considered. In Section 4, we address the possible limitations of the model assumptions made in this investigation and the implications of this study for the promoting effect of water in the catalysis.

3.2. Formic acid adsorption

3.2.1. Infrared Spectroscopy

Spectra for both molecular formic acid and formate were observed when formic acid adsorbed on P25 TiO_2 at room temperature, as shown in Fig. 3. The corresponding assignments (Table 1) were based on a combination of DFT results and previous assignments. The spectrum in Fig. 3 is similar to that reported previously [6,9,12,17–23]. Some studies reported an additional peak at 1413 cm^{-1}, which was assigned to formate [17,19,24]. Peaks at 1787 and 1675 cm^{-1} have been assigned to the C=O stretch of gas phase or physisorbed and chemisorbed formic acid, respectively [9]. The peak at 1105 cm^{-1} has been assigned to CO stretching or CH bending for gas phase or physisorbed formic acid, and the peak at 1263 cm^{-1} has been assigned to CO stretching or CH bending of chemisorbed formic acid [9]. It is noted that OH stretching frequencies for adsorbed hydroxyls have also previously been reported close to 1263 cm^{-1} [25,26]. The peaks at 2945, 2921, and 2867 cm^{-1} correspond to formic acid and formate CH stretching. The large peaks at 1550 and 1378 cm^{-1} correspond to formate COO– asymmetric and symmetric stretching. Previous studies indicated that formic acid adsorbs molecularly on anatase (1 0 1) and dissociatively (to produce formate) on rutile and anatase (0 0 1) [13,27–31]. The most abundant surface of P25 TiO_2 is anatase (1 0 1) [32], which is the most stable anatase surface [14,33–35], but other anatase or rutile surface planes or defects could explain the presence of formate. Gong et al. used DFT to determine that formic acid adsorbs as bidentate formate on anatase (0 0 1) [34].

Table 1
Vibration frequencies from FTIR of formic acid molecularly and dissociatively adsorbed on TiO_2.

Assignments	HCOOH	HCOOH and H_2O
COO and CH Formate	2945	2945
CH Formic Acid	2921	2921
CH Formate	2867	2861
C=O p-Formic Acid	1787	
c-Formic	1675	
COO- asym, Formate	1550	1565
COO- sym, Formate	1378	1360
COO- sym, Formate	1360	1360
CH Formate	1323	1323
CO or CH c-Formic Acid	1263	
CO or CH p-Formic Acid	1105	

c denotes chemisorbed and p denotes physisorbed.

Adsorption geometries of formate are identified by examining the frequency difference between COO– asymmetric and symmetric stretches, denoted as $\Delta\nu_{as\text{-}s}$, relative to the aqueous ionic formate ($\Delta\nu_{ionic} = 201$ cm^{-1}) [18,36–40]. Aqueous ionic formate peaks for COO– asymmetric and symmetric stretching are at 1567 and 1366 cm^{-1} [18]. The correlations between $\Delta\nu_{as\text{-}s}$ and adsorption geometry have been described as follows [39,40].

$\Delta\nu_{as\text{-}s} > \Delta\nu_{ionic}$: monodentate coordination.
$\Delta\nu_{as\text{-}s} < \Delta\nu_{ionic}$: chelating or bidentate bridging.
$\Delta\nu_{as\text{-}s} \ll \Delta\nu_{ionic}$: bidentate chelating.

The $\Delta\nu_{as\text{-}s}$ was 172 cm^{-1} in Fig. 3, indicating that monodentate formate was not on the surface. The bridging and chelating modes cannot be distinguished from IR spectra. Previous computational studies determined that the chelating formate structure is less stable then the bidentate bridging structure [14,27]. Thus, apparently formate adsorbs in the bidentate bridging configuration on P25 TiO_2 at room temperature.

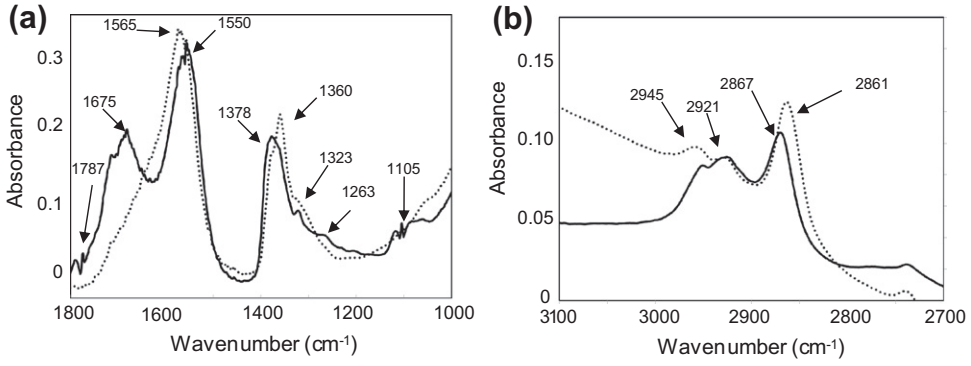

Fig. 3. Infrared spectra of formic acid and water on P25 TiO_2 at room temperature: (a) from 1000 to 1800 cm^{-1}, (b) from 2700 to 3100 cm^{-1}. The solid line shows a spectrum collected after a saturating exposure of formic acid, and the dotted line shows a spectrum collected after water addition to the formic acid saturated surface.

3.2.2. Temperature-programmed desorption

Formic acid was adsorbed to saturation coverage on TiO_2, and TPD results showed 52 μmol g^{-1} of formic acid desorbed in a broad peak at 428 K and a smaller peak at 525 K (Fig. 4). Most of the formic acid decomposed to form 306 μmol g^{-1} H_2O, which desorbed in peaks at 468 and 525 K, and 450 μmol g^{-1} CO, which desorbed in overlapping peaks at 488, 525, and 570 K (Fig. 5). Kim et al. and Muggli et al. identified the same desorption products for formic acid TPD, but with a different number of desorption peaks and slightly different temperatures. On P25 TiO_2, Kim et al. [41] observed formic acid and water desorption peaks at 400 K and attributed CO and H_2O desorption peaks at 525 and 600 K to formate decomposition. From another study on the anatase (0 0 1), formic acid and water desorbs at 390 K, and the remaining formate decomposes to CO and H_2O in a single peak at 570 K [42]. Muggli et al. observed that formic acid desorbs and dehydrates to CO and H_2O in a single peak at 525 K on P25 TiO_2 [43].

3.3. Effect of water on formic acid adsorption

3.3.1. Infrared spectroscopy

Infrared studies show that water displaced formic acid and changed the formate adsorption geometry on P25 TiO_2. When water was added at its room-temperature saturation pressure to the IR cell, the formic acid peaks decreased and the formate COO– symmetric and asymmetric peaks shifted and increased in amplitude (Fig. 3, dashed line). Chemisorbed formic acid peaks at 1675 and 1263 cm^{-1} and physisorbed formic acid peaks at 1787

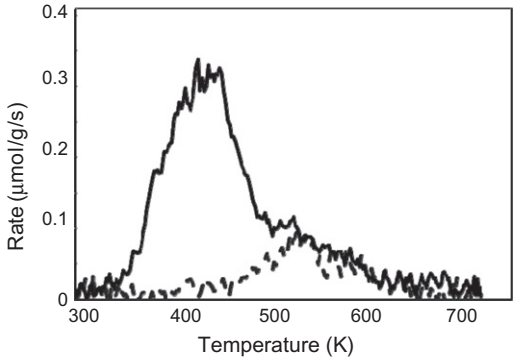

Fig. 4. Formic acid TPD recorded after formic acid and water adsorption on P25 TiO_2. The solid line shows a spectrum collected after a saturating exposure of formic acid, and the dashed line shows a spectrum collected after water addition to the formic acid saturated surface.

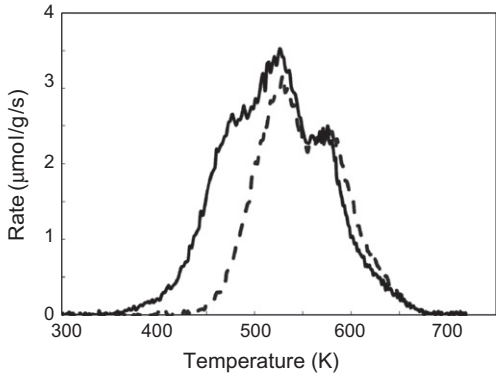

Fig. 5. Carbon monoxide TPD recorded after formic acid and water adsorption on P25 TiO_2. The solid line shows a spectrum collected after a saturating exposure of formic acid, and the dashed line shows a spectrum collected after water addition to the formic acid saturated surface.

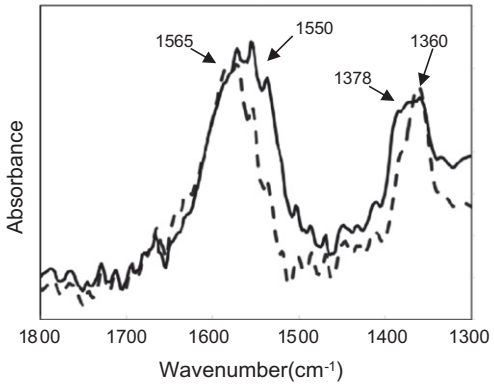

Fig. 6. Infrared spectra of formic acid and water on P25 TiO_2. The dashed line shows a spectrum collected after water addition to the formic acid saturated surface, and the solid line shows a spectrum collected after heating that surface to 383 K.

and 1105 cm^{-1} decreased. Due to the large intensity of the OH stretching peak for water, changes in the high-frequency region are difficult to discern. The COO– asymmetric peak shifted from 1550 to 1565 cm^{-1}, and the COO– symmetric peak shifted from 1378 to 1360 cm^{-1}; these changes increased the $\Delta\nu_{as\text{-}s}$ from 170 to 210 cm^{-1}. The CH formate peak at 2867 cm^{-1} also shifted slightly to 2861 cm^{-1}. Vibrational calculations from DFT, described in a separate contribution [44], and previous literature aided in interpreting the peak shifts. Heating the sample to 383 K removed all the adsorbed water, and largely reversed the COO– asymmetric and symmetric peak shifts. The formate peak at 1565 cm^{-1} shifted back to 1550 cm^{-1}, the frequency observed before the water addition, and the peak at 1360 cm^{-1} broadened to include a smaller peak at 1378 cm^{-1}, as shown in Fig. 6.

The changes in the vibrational spectrum associated with formate after dosing of water suggest a change in the structure of the coadsorbate. One possible transition consistent with the higher reactivity of the water-dosed surface is the conversion of bidentate formate to a solvated form of monodentate formate, the latter of which has been found to be more reactive toward decomposition in prior investigations on model surfaces. This possibility is explored in more detail in a separate contribution [44].

3.3.2. Temperature-programmed desorption

The TiO_2 surface was saturated with formic acid and then exposed to 5 μL of water. The water displaced 70 ± 7% of the formic acid that otherwise would have desorbed intact during TPD (Fig. 4). Water displaced the weakly adsorbed formic acid, so that the rest that desorbed intact had a peak temperature of 525 K. Thirty percent less CO desorbed after water adsorption, and the CO peak at 488 K was absent, whereas the other two CO peaks were unchanged (Fig. 5). The CO peak temperatures did not shift because monodentate formate reverted to bidentate formate above 383 K, as seen from IR results (Fig. 6). The water peak temperature did not change, but the amount desorbed increased to 326 μmol g^{-1}. The water increase, 20 μmol g^{-1}, is comparable to the formic acid decrease, 36 μmol g^{-1}. Even though formic acid competes for sites favorably with water, it can be displaced if formic acid is not in the vapor phase. Henderson et al. [2] reported that water removes acetone from rutile TiO_2, even though acetone adsorbs more strongly than water.

4. Discussion

This discussion will relate the results presented above to observations of the promotional effects of water on photocatalysis.

Photocatalytic decomposition of formic acid forms CO_2 and H_2O on TiO_2, but it forms CO_2 and H_2 on Pt/TiO_2. The reaction steps for formic acid PCD on TiO_2 and Pt/TiO_2 are listed below in Eq. (4.1)–(4.7).

$$HCOOH \leftrightarrow HCOOH(s) \tag{4.1}$$

$$HCOOH(s) \leftrightarrow H(s) + HCOO(s) \tag{4.2}$$

$$HCOO(s) \leftrightarrow CO_2 + H(s) \tag{4.3}$$

$$2H(s) + O(\text{lattice}) \rightarrow H_2O(s) \tag{4.4}$$

$$H_2O(s) \leftrightarrow H_2O \tag{4.5}$$

$$H(s) \leftrightarrow H(Pt) \tag{4.6}$$

$$2H(Pt) \leftrightarrow H_2 \tag{4.7}$$

In the above equations, (s) denotes a species adsorbed on TiO_2 and (Pt) denotes a species adsorbed on Pt. Thus, during formic acid PCD on TiO_2, formic acid extracts a lattice oxygen from TiO_2 to produce CO_2 and H_2O at room temperature. This creates an oxygen vacancy that decreases the PCD rate [45,46]. Based on findings by Muggli et al., [45], the rate-limiting step for formic acid PCD on TiO_2 is likely the extraction of lattice oxygen. They saw a large rate decrease during PCD, but after a period of dark time that replenished the oxygen lattice, the rate increased. Muggli et al. concluded that lattice oxygen extraction causes the slow deactivation of TiO_2. Water did not re-oxidize TiO_2 in their experiments, even during UV illumination. One possible reason for the higher PCD rate on Pt/TiO_2 is that formic acid decomposition does not require lattice oxygen removal since H_2 forms through Eq. (4.7) preferentially over H_2O formation by Eq. (4.5). The Pt acts as a site for hydrogen atoms to recombine to H_2, which then desorbs. The rate-limiting step for formic acid PCD on Pt/TiO_2 would then likely be either formic acid or formate decomposition because formic acid adsorption (Eq. (4.1)) and H_2 formation on Pt (Eq. (4.7)) are rapid [47].

Water has varying effects on steps 4.1–4.7. The reaction mechanism on TiO_2 and Pt/TiO_2 are the same through Eq. (4.3), and thus water would have the same effect on steps 4.1–4.3 on Pt/TiO_2. From IR and TPD, water displaces formic acid on TiO_2, making the adsorption of formic acid in step 4.1 more difficult. Water may increase the decomposition rate of formic acid to formate (Eq. (4.2)), as suggested by the DFT calculations of Vittadini et al. [14]. Water may also speed up formate decomposition (Eq. (4.3)). The IR studies showed that water appeared to perturb the structure of adsorbed formate, perhaps to a more reactive form, e.g., through the conversion of bidentate formate to monodentate formate as shown in step 4.8, with monodentate formate being more reactive, as discussed below:

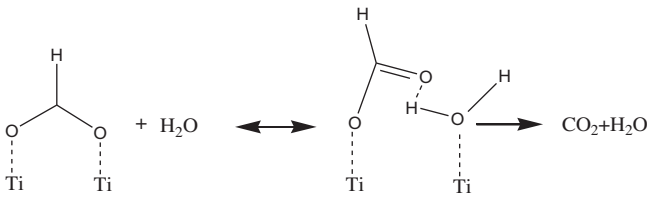

(4.8)

On TiO_2, Muggli and Falconer determined that water does not affect the rate of lattice oxygen extraction (Eq. (4.4)), [45] and the desorption of water (Eq. (4.5)) is rapid. On Pt/TiO_2, water may increase the hydrogen transport rate to Pt (Eq. (4.6)) if the hydrogen recombination rate is diffusion limited. Water's effect on the hydrogen recombination rate and desorption from Pt (Eq. (4.7)) was not investigated, but this step is sufficiently fast that it should not be rate limiting. Finally, it is important to note that rate acceleration could be caused by the participation of species not directly invoked in the reaction scheme shown above. For example, previous studies have shown that UV exposure causes water to form hydroxyl radicals that may accelerate the reaction [48,49]. The possible importance of hydroxyls in this surface chemistry is further underscored by computational studies reported elsewhere [44].

From characterization experiments and DFT calculations reported previously by Vittadini et al., water appears to influence both formic acid dissociation and formate decomposition on TiO_2. There may be a larger effect on Pt/TiO_2 because the rate-limiting step is formic acid or formate decomposition, and on TiO_2 it is the extraction of lattice oxygen. Liao et al. [9] reported that formic acid PCO was 53 times faster than formate PCO. This indicates the effect of water on formate decomposition may have a greater effect on the overall rate of PCD.

The possible higher reactivity of monodentate carboxylates is supported by several previous studies. Henderson et al. [50] determined that monodentate carboxylates are more reactive then bidentate carboxylates on TiO_2 (1 1 0). Using FTIR, Wu et al. [51] showed that the monodentate PCO rate is 1.5 times higher than the bidentate formate PCO rate for methoxy and ethoxy groups. These results are consistent with an accelerated reaction rate resulting from the conversion of bidentate formate to monodentate formate. Also, Miura et al. [52] determined that formate decomposes on NiO (1 1 1) by first changing from bidentate to monodentate, then formate rotating around the CO axis, and finally hydrogen atom transferring from the formate to the surface atom. If formate decomposes by the same mechanism on TiO_2, the increased conversion by water from bidentate to monodentate formate would increase the rate of formate decomposition.

5. Conclusions

Transient reaction studies showed that physisorbed water dramatically increased the rate of photocatalytic decomposition (PCD) on Pt/TiO_2 and mildly increased the PCD rate on TiO_2, whereas chemisorbed water did not. Infrared spectroscopy showed both molecular formic acid and bidentate formate on P25 TiO_2 at room temperature. Water displaced formic acid and shifted formate COO– asymmetric and symmetric peaks, indicating a transition from bidentate formate to monodentate formate. This transition may relate to the increase in PCD rate.

Acknowledgment

We gratefully acknowledge support by the National Science Foundation, Grant CBET0730047.

References

[1] A.L. Linsebigler, G.Q. Lu, J.T. Yates, Chem. Rev. 95 (1995) 735.
[2] M.A. Henderson, J. Catal. 256 (2008) 287.
[3] L.F. Liao, C.F. Lien, D.L. Shieh, M.T. Chen, J.L. Lin, J. Phys. Chem. B 106 (2002) 11240.
[4] S. Sato, JCS-Chem. Comm. (1982) 26.
[5] S. Sato, J. Phys. Chem. 87 (1983) 3531.
[6] M. El-Maazawi, A.N. Finken, A.B. Nair, V.H. Grassian, J. Catal. 191 (2000) 138.
[7] T.N. Obee, S.O. Hay, Environ. Sci. Technol. 31 (1997) 2034.
[8] C. Hagglund, B. Kasemo, L. Osterlund, J. Phys. Chem. B 109 (2005) 10886.
[9] L.F. Liao, W.C. Wu, C.Y. Chen, J.L. Lin, J. Phys. Chem. B 105 (2001) 7678.
[10] S. Sato, K. Ueda, Y. Kawasaki, R. Nakamura, J. Phys. Chem. B 106 (2002) 9054.
[11] D.S. Muggli, J.L. Falconer, J. Catal. 187 (1999) 230.
[12] T. Chen, G.P. Wu, Z.C. Feng, G.S. Hu, W.G. Su, P.L. Ying, C. Li, Chin. J. Catal. 29 (2008) 105.
[13] H. Idriss, A. Miller, E.G. Seebauer, Catal. Today 33 (1997) 215.
[14] A. Vittadini, A. Selloni, F.P. Rotzinger, M. Gratzel, J. Phys. Chem. B 104 (2000) 1300.
[15] A. Larson, J.A. Widegren, J.L. Falconer, J. Catal. 157 (1995) 611.
[16] D.S. Muggli, S.A. Keyser, J.L. Falconer, Catal. Lett. 55 (1998) 129.

[17] T. Kecskes, J. Rasko, J. Kiss, Appl. Catal. A 268 (2004) 9.
[18] J.R.S. Brownson, M.I. Tejedor-Tejedor, M.A. Anderson, J. Phys. Chem. B 110 (2006) 12494.
[19] Z.Q. Yu, S.S.C. Chuang, J. Catal. 246 (2007) 118.
[20] R.C. Millikan, K.S. Pitzer, JCS 80 (1958) 3515.
[21] T. van der Meulen, A. Mattson, L. Osterlund, J. Catal. 251 (2007) 131.
[22] C.C. Chuang, W.C. Wu, M.C. Huang, I.C. Huang, J.L. Lin, J. Catal.185 185 (1999) 423.
[23] G.Y. Popova, T.V. Andrushkevich, Y.A. Chesalov, E.S. Stoyanov, Kinet. Catal. 41 (2000) 805.
[24] C.-C. Chuang, W.-C. Wu, M.-C. Huang, I.C. Huang, J.-L. Lin, J. Catal. 185 (1999) 423.
[25] A. Yee, S.J. Morrison, H. Idriss, J. Catal. 186 (1999) 279.
[26] J.L. Davis, M.A. Barteau, Surf. Sci. (1990) 235.
[27] P.R. McGill, H. Idriss, Surf. Sci. 602 (2008) 3688.
[28] H. Uetsuka, M.A. Henderson, A. Sasahara, H. Onishi, J. Phys. Chem. B 108 (2004) 13706.
[29] M.A. Henderson, J. Phys. Chem. B 101 (1997) 221.
[30] B.E. Hayden, A. King, M.A. Newton, J. Phys. Chem. B 103 (1998) 203.
[31] Y. Uemura, T. Taniike, M. Tada, Y. Morikawa, Y. Iwasawa, J. Phys. Chem. C 111 (2007) 16379.
[32] J.F. Porter, Y.-G. Li, C.K. Chan, J. Mater. Sci. 34 (1999) 1523.
[33] A. Vittadini, A. Selloni, F.P. Rotzinger, M. Gratzel, Phys. Rev. Lett. 81 (1998) 2954.
[34] X.Q. Gong, A. Selloni, A. Vittadini, J. Phys. Chem. B 110 (2006) 2804.
[35] A. Tilocca, A. Selloni, J. Phys. Chem. B 108 (2004) 4743.
[36] J.R.S. Brownson, M.I. Tejedor-Tejedor, M.A. Anderson, Chem. Mater. 17 (2005) 6304.
[37] F.P. Rotzinger, J.M. Kesselman-Truttmann, S.J. Hug, V. Shklover, M. Gratzel, J. Phys. Chem. B 108 (2004) 5004.
[38] I. Dolamic, T. Burgi, J. Phys. Chem. B 110 (2006) 14898.
[39] G.B. Deacon, F. Huber, R.J. Phillips, Inorg. Chim. Acta 104 (1985) 41.
[40] G.B. Deacon, R.J. Phillips, Coordin. Chem. Rev. 33 (1980) 227.
[41] K.S. Kim, M.A. Barteau, Langmuir 4 (1988) 945.
[42] K.S. Kim, M.A. Barteau, Langmuir 6 (1990) 1485.
[43] D.S. Muggli, J.T. McCue, J.L. Falconer, J. Catal. 173 (1998) 470.
[44] K.L. Miller, J.W. Medlin, J.L. Falconer, J. Catal. (2010), submitted for publication.
[45] D.S. Muggli, J.L. Falconer, J. Catal. 191 (2000) 318.
[46] G.D. Lee, J.L. Falconer, Catal. Lett. 70 (2000) 145.
[47] K. Mogyorosi, A. Kmetyko, N. Czirbus, G. Vereb, P. Sipos, A. Dombi, React. Kinet. Catal. Lett. 98 (2009) 215.
[48] K. Takahashi, H. Yui, J. Phys. Chem. C 113 (2009) 20322.
[49] J. Peral, X. Domènech, D.F.J. Ollis, Chem. Technol. Biotechnol. 70 (1997) 117.
[50] M.A. Henderson, J.M. White, H. Uetsuka, H. Onishi, J. Catal. 238 (2006) 153.
[51] W.C. Wu, C.C. Chuang, J.L. Lin, J. Phys. Chem. B 104 (2000) 8719.
[52] T. Miura, H. Kobayashi, K. Domen, J. Phys. Chem. B 105 (2001) 10001.